Available online at www.sciencedirect.com
ScienceDirect
Catalysis Today 119 (2007) 267–272
CATALYSIS TODAY
www.elsevier.com/locate/cattod

Simultaneous removal of NO_x and diesel soot particulates over nanometric $La_{2-x}K_xCuO_4$ complex oxide catalysts

Jian Liu, Zhen Zhao *, Chun-ming Xu, Ai-jun Duan, Tao Meng, Xiao-jun Bao

State Key Laboratory of Heavy Oil Processing, China University of Petroleum, Beijing 102249, China

Available online 7 September 2006

Abstract

The nanometric $La_{2-x}K_xCuO_4$ oxide catalysts with K_2NiF_4-type structure were prepared by auto-combustion method using citric acid as a ligand and an adjusting agent of particle-size and morphology. The structures and physico-chemical properties of these perovskite-like oxides were examined by means of XRD, FT-IR, H_2-TPR and chemical analysis. The catalytic activities for the simultaneous removal of soot and NO_x were evaluated by a technique of the temperature-programmed oxidation reaction (TPO). In the $La_{2-x}K_xCuO_4$ catalysts, the partial substitution of K for La at A-site leads to the increase of the concentrations of Cu^{3+} and oxygen vacancy. Thus, it enhances the catalytic activity for simultaneous removal of NO_x and diesel soot, and the optimal substitution amount of potassium x is equal to 0.5 among these samples. T_{10}, T_{50}, T_{90} are 376, 438, 487 °C and P_{N_2} is 22%, respectively, for simultaneous removal of NO_x and soot particulates over the $La_{1.5}K_{0.5}CuO_4$ catalyst under loose contact conditions between the catalyst and soot.

Keywords: Nanometer; La–K–Cu perovskite-like oxides; Diesel soot; NO_x; Simultaneous removal

1. Introduction

The deleterious effect on human health of particulate matters (PMs) and NO_x presented in the diesel exhaust gases has attracted great concerns, and resulted in the formulation of restrictive legislation both in the EU and the US. Since the reduction of both PM and NO_x emissions to the permitted level cannot be accomplished by engine modifications alone, after-treatment processes for the simultaneous reduction of their emissions from diesel exhaust should be developed [1–3]. As one possible process, Yoshida et al. proposed the simultaneous catalytic conversion of PM and NO_x into CO_2 and N_2 in an oxidizing atmosphere by using catalyzed soot traps [4]. Although this method involves many technological difficulties to be overcome (the development of efficient and thermally stable traps, the contact between catalyst and trapped soot, etc.), the active catalyst is considered to be the most important one [5].

Several authors [5–10] reported that perovskite and spinel oxides are active for simultaneous NO_x-soot removal reaction. In addition, the substitutional incorporation of alkali metal into A-sites of perovskite-type (ABO_3) oxides was found to be quite effective in enhancing the activity and selectivity for the NO_x–O_2-soot reaction [6–9]. Teraoka et al. found that La–K–Mn–O perovskite-type oxides are good candidate catalysts for diesel soot combustion [10], but they reported the relevant catalytic activities under tight contact conditions between the catalysts and PM particle. However, it is often a loose contact between the catalysts on the surface of filter and PM particle under practical conditions [11,12]. Thus, it is rather significant to study and design the active catalysts for soot particulate oxidation under loose contact conditions.

Application of catalyst materials depends on their size and morphology [13]. Therefore, much emphasis has been laid on the shape and size control recently [14]. The surface particle sizes of nanometer material are small. Surface atoms on the surface of nanometer catalysts have extra and high surface energies and they are good at mobility, therefore the contact is still very good between catalysts and soot even under loose contact conditions. In the present study, the nanometer $La_{2-x}K_xCuO_4$ complex

* Corresponding author. Tel.: +86 10 8973 1586; fax: +86 10 69724721.
E-mail address: zhenzhao@cup.edu.cn (Z. Zhao).

0920-5861/$ – see front matter © 2006 Elsevier B.V. All rights reserved.
doi:10.1016/j.cattod.2006.08.040

oxides were prepared by the auto-combustion method, and it was investigated that the substitution amounts of A-site cation affect on the structure and catalytic performances for soot particle combustion under loose contact conditions. The probable reasons that can lead to the activity enhancement for the K-substitution samples compared to the unsubstitution sample were discussed.

2. Experimental

2.1. Catalyst preparation

A series of $La_{2-x}K_xCuO_4$ ($x = 0$, 0.1, 0.2, 0.3, 0.4, 0.5, 0.6) complex oxides with K_2NiF_4-type structure were prepared by the auto-combustion method. The corresponding metal nitrates were used as starting materials for obtaining an aqueous solution of La^{3+}, K^+ and Cu^{2+} with appropriate stoichiometry. A solution of citric acid (100%) in excess was chosen as a ligand and an adjusting agent of particle-size and morphology. The resulting solution was heated at flow air atmosphere by a electric furnace with 2 kW power and evaporated to dryness with vigorous stirring, following burning or explosion and finally the precursor was calcined at 800 °C for 4 h in a static air.

2.2. Catalyst characterization

The crystal structures of the fresh catalysts were determined by a powder X-ray diffractometer (Shimadzu XRD 6000), using Cu Kα ($\lambda = 0.1542$ nm) radiation combined with Nickel filter operating at 40 kV and 10 mA. The diffractometer data were recorded for 2θ values between 15 and 80° at a scanning rate of 4 ° min^{-1}. The patterns were compared with JCPDS reference data for phase identification. The Scherrer equation was used to calculate the crystal size of the studied samples.

FT-IR absorbance spectra were obtained in the wave number ranging between 6000 and 400 cm^{-1} via a FTS-3000 spectrophotometer manufactured by American Digilab company. The measured wafer was prepared as KBr pellet with the weight ratio of sample to KBr, 1/100. The resolution was set at 2 cm^{-1} during measurement.

TPR measurements were performed in a conventional flow apparatus. Two hundred milligram sample was pretreated at an oxygen atmosphere by calcination at 600 °C for 1 h and subsequently cooled to 100 °C with helium flowing. Afterwards, the TPR was carried out using 10% hydrogen in helium at constant flow rate of 40 cm^3 min^{-1}, from 100 °C to 900 °C at a heating rate of 10 °C min^{-1}. The hydrogen consumption signal was monitored by a thermal conductivity detector (TCD). Before the outlet gases entering the TCD, a cooling trap and a filter packed with molecular sieve 5A (60–80 meshes) were used to remove H_2O and CO_2.

2.3. Catalytic activity measurement

The catalytic activities of the prepared samples were evaluated with a TPO reaction. The reaction temperature varied during each TPO run from 200 °C to 600 °C at a 2 °C min^{-1} rate. Printex-U was used as model soot and 180 mg mixture of catalyst and soot (5:1, w/w) was placed in the tubular quartz reactor (Ø = 10 mm). The catalyst and soot were mixed with a spatula in order to reproduce the loose contact mode, which is the most representative model of diesel particles flowing through a catalytic filter [11]. The occurrence of heat and mass transfer limitations would influence the observed reaction rates. In addition, it was also found to influence soot combustion temperatures about 0–5 °C. In order to accurately detect the true reaction temperatures, the catalyst-soot fixed bed was sandwiched between two quartz-wool layers. And the tip of a K-type thermocouple was located well inside the catalyst bed itself. The reaction temperature was controlled through a PID-regulation system based on the measurements of an external K-type thermocouple. Reactant gases containing 5% O_2 and 2000 ppm NO balanced with He were passed through a mixture of the catalyst and soot at a flow rate of 50 ml min^{-1}. The outlet gas composition from the reactor passed through a 1 cm^3 sampling loop of a six-point gas-sampling valve before it was being injected into an on-line gas chromatograph (GC). The GC with both a thermal conductivity detector and a flame ionization detector (FID) was used to analyze the gaseous mixture. The TCD was used to measure the concentration of O_2, N_2, CO, NO after separating these gases over a molecular sieve 5A column. The FID was employed to determine CO and CO_2 concentrations after separating these gases over a Porapak N column and converting them to methane over a Ni catalyst at 380 °C. The selectivity to CO_2 formation (S_{CO_2}) was defined as that the CO_2 outlet concentration (C_{CO_2}) divided by the sum of the CO_2 and CO outlet concentration, i.e., $S_{CO_2} = C_{CO_2}/(C_{CO} + C_{CO_2})$. The catalytic activity was evaluated by the values of T_{10}, T_{50}, and T_{90}, which were defined as the temperatures at which 10, 50, and 90% of the soot, respectively, were oxidized during the TPO procedure. For purifying the exhaust gases from diesel engines, nitrogen oxides should be converted into N_2. Thus, the productivity of N_2, i.e., P_{N_2} is another important parameter. In this work, N_2 exclusively derived from the conversion of NO due to the NO being the only nitrogen containing gas in the inlet gaseous components. Therefore, P_{N_2} equals to the double of outlet nitrogen concentration divided by the inlet NO concentration, i.e., $P_{N_2} = 2[N_{2out}]/[NO_{in}]$.

3. Results and discussion

3.1. Defect structure of $La_{2-x}K_xCuO_4$

In the series of $La_{2-x}K_xCuO_4$ oxides, the deficient positive charge resulting from the substitution of K^+ for La^{3+} could be balanced either by the formation of higher oxidation state ion at B-site, i.e., $Cu^{2+} \rightarrow Cu^{3+}$, or by the formation of oxygen vacancy (V_o). In fact, the two cases often occur at the same time. The average valence of Cu ions and the contents of Cu^{3+} or Cu^{2+} in the series of oxides were determined by the chemical analysis using the method of iodometry [15]. The oxygen nonstoichiometry (λ) was calculated on the assumption that copper is present as a mixture of Cu^{3+} and Cu^{2+} in $La_{2-x}K_xCuO_4$ system and other elements are present as La^{3+}, K^+, and O^{2-}, respectively [5]. The variation of the average valence of Cu ions, λ and the Cu ion

Table 1
The average valence of Cu ions, nonstiochiometric oxygen (λ) and the Cu ions content in the $La_{2-x}K_xCuO_4$ system (wt.%) ($x = 0, 0.1, 0.2, 0.3, 0.4, 0.5, 0.6$)

Catalysts	Cu^{2+}/wt.%	Cu^{3+}/wt.%	Cu^{3+}/Cu^{2+}	Average valence of Cu	Nonstiochiometric oxygen (λ)
$La_{1.4}K_{0.6}CuO_4$	0.1983	0.0024	0.0123	2.0113[a]	−0.1824
$La_{1.5}K_{0.5}CuO_4$	0.1852	0.0025	0.0137	2.0135[a]	−0.1932
$La_{1.6}K_{0.4}CuO_4$	0.1730	0.0081	0.0471	2.0449[a]	−0.1775
$La_{1.7}K_{0.3}CuO_4$	0.1315	0.0270	0.2053	2.1703	−0.1148
$La_{1.8}K_{0.2}CuO_4$	0.1316	0.0241	0.1835	2.1551	−0.1225
$La_{1.9}K_{0.1}CuO_4$	0.1297	0.0213	0.1639	2.1408	−0.0296
La_2CuO_4	0.1488	0.0073	0.0489	2.0467	+0.0233

[a]Represents a approximate value because of impure crystal phase, K_2CO_3 formed.

contents in the $La_{2-x}K_xCuO_4$ system (wt.%) are shown in Table 1. The analysis results show that in the range of $0.0 \leq x \leq 0.3$, the contents of Cu^{3+} increase rapidly and thus, the charge of the mixed oxides is mainly balanced by the increase of Cu^{3+}. In the range of $0.4 \leq x \leq 0.6$, on the other hand, the formation of oxygen vacancies is more pronounced. Cu^{3+} amount is the largest in $La_{1.7}K_{0.3}CuO_4$; however, $La_{1.5}K_{0.5}CuO_4$ has the maximal oxygen vacancy concentration.

3.2. XRD results

The XRD patterns of all the samples give several large diffraction peaks at 31.1°, 47.8° and 33.4°, as shown in Fig. 1, which reveals that the complex oxides of $La_{2-x}K_xCuO_4$ possessed A_2BO_4 perovskite-like type structures [4,5]. When K-substitution amount is equal to or great than 0.4, there is a trace amount of K_2CO_3. Furthermore, Table 2 shows that the average crystal particle size (D) of $La_{2-x}K_xCuO_4$ samples is between 44 and 58 nm. The results reveal that $La_{2-x}K_xCuO_4$ samples prepared by the auto-combustion method possessed nanometer particle sizes.

3.3. FT-IR results

IR characterizing results support the above structure analysis by XRD. As shown in Fig. 2, this series of samples all have the vibration band around 520 and 690 cm^{-1} in the whole range of $0.0 \leq x \leq 0.6$ The former is attributed to the stretching vibration of A–O–B bond in A_2BO_4 type oxide and it is assigned to the vibration mode of A_{2u}. The latter is due to the stretching motion of B–O bond of BO_6 octahedron in the direction of *a*- or *b*-axis, and it belongs to the E_{2u} vibration mode. Compared with the unsubstituted sample La_2CuO_4, the vibration band at ~690 cm^{-1} of K^+-substituted samples become weaker, broader and upshiftting. This result further indicates some amounts of Cu^{2+} changed into Cu^{3+}, which was verified by chemical analysis. Moreover, very weak absorption peaks at 882 and 1060 cm^{-1} appeared in the IR spectra of $La_{2-x}K_xCuO_4$ samples when K-substitution amount exceeded or was equal to 0.4. They are attributed to K–O–C vibration in the K_2CO_3. It should be noteworthy that the small sharp peak near 667 cm^{-1} does not belong to the IR absorption band, and the phenomenon occurs due to the small crystalline particles [16].

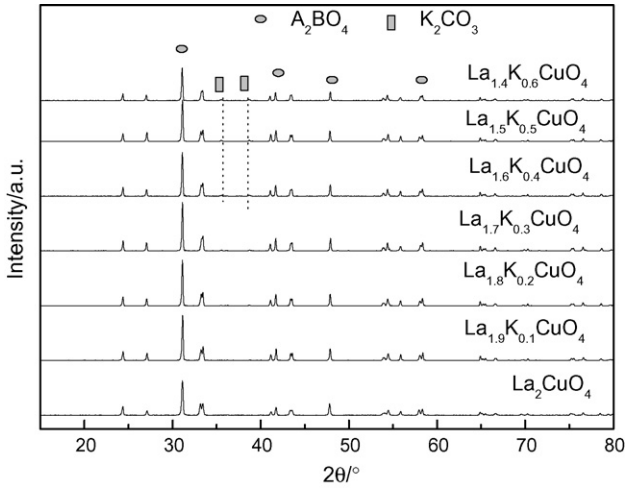

Fig. 1. X-ray diffraction patterns of $La_{2-x}K_xCuO_4$ catalysts ($x = 0, 0.1, 0.2, 0.3, 0.4, 0.5, 0.6$).

3.4. H_2-TPR results

Fig. 3 shows the H_2-TPR profiles of the series of $La_{2-x}K_xCuO_4$ perovskite-like catalysts. During TPR process, not only were the metallic cations with high valence reduced to ions with low valance or metal atoms by H_2, but also the lattice oxygen ion involved the process due to H_2O formed. Therefore, the reducibility of metallic ion and the mobility of lattice oxygen can also be reflected by TPR measurement [17]. There were three kinds of reduction peaks on the TPR curves of all samples, namely, α (150 °C $\leq T \leq$ 450 °C), β (450 °C $\leq T \leq$ 700 °C), γ ($T \geq$ 700 °C). Spencci and Tofanari demonstrated that the α could be referred to a less negatively charged species O_2^-, β to a more negatively charged species O^- and γ to the lattice oxygen [18]. After the samples were reduced by H_2 at 700 °C, the

Table 2
The average crystal size of $La_{2-x}K_xCuO_4$ catalysts ($x = 0, 0.1, 0.2, 0.3, 0.4, 0.5, 0.6$)

Catalysts	Crystal surface	I/I1	2θ	β (radian)	D (nm)
La_2CuO_4	311	100	31.1184	0.0032	43.88
$La_{1.9}K_{0.1}CuO_4$	311	100	31.14	0.0027	52.62
$La_{1.8}K_{0.2}CuO_4$	311	100	31.1165	0.0025	57.51
$La_{1.7}K_{0.3}CuO_4$	311	100	31.1202	0.0024	58.29
$La_{1.6}K_{0.4}CuO_4$	311	100	31.1096	0.0026	54.88
$La_{1.5}K_{0.5}CuO_4$	311	100	31.1224	0.0027	52.35
$La_{1.4}K_{0.6}CuO_4$	311	100	31.1233	0.0029	50.03

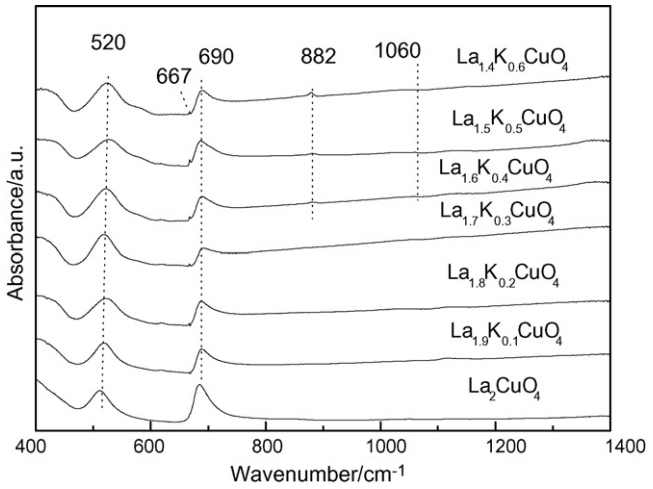

Fig. 2. The FT-IR spectra of $La_{2-x}K_xCuO_4$ catalysts ($x = 0$, 0.1, 0.2, 0.3, 0.4, 0.5, 0.6).

structure analysis with IR was carried out. The result (not be shown for concision) shows that the K_2NiF_4-type structure is still retained after the reduction was carried out till the temperature corresponding to α and β peaks, which are lower than 700 °C. Owing to a large amount of oxygen vacancies existing in the structure of samples, oxygen will be absorbed after the samples are pretreated in the oxygen atmosphere. So α could be attributed to the following reaction: $Cu^{3+} + O_2^- + 2H_2 \rightarrow Cu^{2+} + 2H_2O$, and β could be ascribed to the following reduction process: $Cu^{3+} + O^- + H_2 \rightarrow Cu^{2+} + H_2O$. IR results also show that the K_2NiF_4-type structures of the catalysts were destroyed after their reductions were carried out till the temperature (900 °C) corresponding to γ peak, and the colors of all the samples transformed into red or light red after they were reduced in H_2 atmosphere at 900 °C. It reveals that Cu^{2+} ions were reduced into red Cu_2O (Cu^+) because the metal Cu is not red but black under the condition of high dispersion. In addition, Cu_2O was of high stability in H_2 atmosphere even if at 900 °C. It indicates that γ reduction peak corresponded to the reduction process:

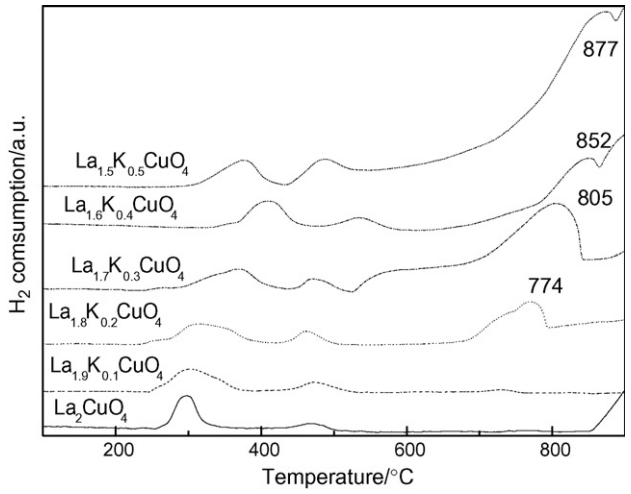

Fig. 3. The H_2-TPR profiles of $La_{2-x}K_xCuO_4$ catalysts ($x = 0$, 0.1, 0.2, 0.3, 0.4, 0.5).

Table 3
The catalytic performances of $La_{2-x}K_xCuO_4$ catalysts for simultaneous removal of soot and NO ($x = 0$, 0.1, 0.2, 0.3, 0.4, 0.5, 0.6)

Catalysts	T_{10} (°C)	T_{50} (°C)	T_{90} (°C)	S_{CO_2} (%)	P_{N_2} (%)
La_2CuO_4	457.5	517.7	546.5	94.5	10.3
$La_{1.9}K_{0.1}CuO_4$	421.4	510.6	558.5	87.7	17.3
$La_{1.8}K_{0.2}CuO_4$	392.6	469.8	511.0	92.4	15.4
$La_{1.7}K_{0.3}CuO_4$	390.7	463.0	500.8	92.6	16.4
$La_{1.6}K_{0.4}CuO_4$	376.0	445.6	489.7	92.9	19.3
$La_{1.5}K_{0.5}CuO_4$	376.0	438.0	487.2	98.5	21.6
$La_{1.4}K_{0.6}CuO_4$	379.6	446.8	491.4	96.4	20.1

$2Cu^{2+} + 2O^{2-} + H_2 \rightarrow Cu_2O + H_2O$. According to the temperature ranges of α, β and γ peaks, it seems that O_2^- and O^- should be directly responsible for the soot combustion.

3.5. The results of catalytic activity measurements

In the practical case, the soot abatement should occur on a filter in combination with the highly active catalyst under a flow condition. Because of the experimental difficulty to supply the solid soot continuously to the reaction system, the reactions have been exclusively investigated by the TPO technique in which a mixture of a catalyst and soot is heated in gaseous reactants. Thus, the experimental results were unable to directly apply to a practical diesel vehicle. The soot conversion was calculated by integration of CO and CO_2 concentrations over the recorded time intervals that were always equal to 200 min because of each TPO running from 200 to 600 °C at a 2 °C min^{-1} rate. The amount of CO and CO_2 were added and multiplied by the gas velocity (50 ml min^{-1}), converted from ml to mg "*C*", and divided by the amount of soot initially present. The carbon balance was always close to 99%.

Table 3 and Fig. 4 shows the TPO data for the simultaneous removal NO_x and soot. The outlet gaseous components only CO_2 and N_2 are plotted for the sake of clarity. From these data it can be seen that the changes showed the same trends for T_{10}, T_{50}, T_{90}, S_{CO_2} and P_{N_2}. The peaks of CO_2 and N_2 production in all TPO tests performed on the pervious samples were quite close. In other words, soot combustion and NO_x reduction take place simultaneously on the selected catalysts. In the $La_{2-x}K_xCuO_4$ catalysts, the partial substitution of K for La at A-site greatly enhanced the catalytic activity for simultaneous removal of NO_x and diesel soot. The optimal substitution amount of K (x) was equal to 0.5 for reduction of NO_x and soot combustion among these samples under loose contact conditions between the catalyst and soot.

3.6. The controlling factors for simultaneous removal of NO_x and diesel soot

It is a complicated gas-solid-solid multi-phase reaction process for simultaneously catalytic removal of soot and NO_x. The TPO results demonstrate that the $La_{2-x}K_xCuO_4$ perovskite-like complex oxides are good candidate catalysts for simultaneously catalytic removal of NO_x and diesel soot particulates. The following three reasons can lead to the activity

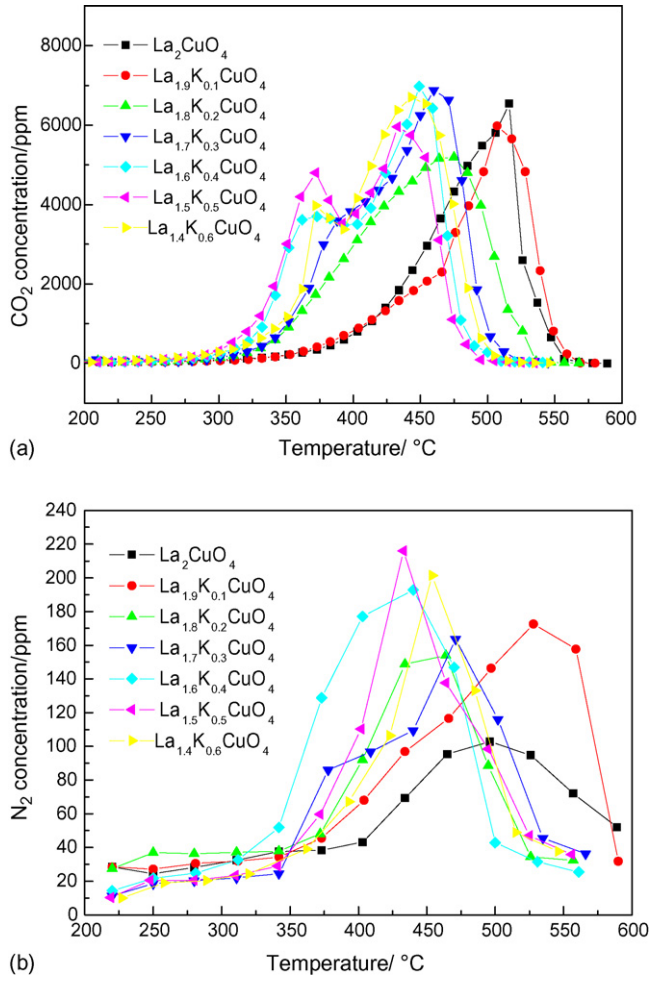

Fig. 4. The outlet CO_2 and N_2 concentration profiles during TPO over $La_{2-x}K_xCuO_4$ catalysts ($x = 0$, 0.1, 0.2, 0.3, 0.4, 0.5, 0.6): (a) outlet CO_2 concentration profiles and (b) outlet N_2 concentration profiles.

enhancement for K-substitution samples compared to the unsubstituted sample (La_2CuO_4). The first one is that A-site cation (La^{3+}) are partly replaced by K^+ and partial Cu^{2+} changed to Cu^{3+}, which had better catalytic oxidation activity than Cu^{2+}. Therefore, it can lower the temperature of soot combustion. However, for the series of $La_{2-x}K_xCuO_4$ catalysts, the Cu^{3+} increases rapidly but the catalytic activity toward NO_x reduction enhances slowly in the range of $0.1 \leq x \leq 0.3$ with increasing x. It reveals that Cu^{3+} has a rather negligible effect on P_{N_2}. The second one is the increase in the content of oxygen vacancy (V_o) in $La_{2-x}K_xCuO_4$. The presence of a large amount of oxygen vacancies would enhance the adsorption and activation of NO or molecular oxygen at catalyst surface. Therefore, it can improve the catalytic activity for the simultaneous removal of NO_x and soot. As shown in Tables 1 and 3, there is a good consistence between the nonstoichiometric oxygen content and the catalytic activity. Furthermore, Fig. 3 shows that the areas of H_2-TPR reduction peak increase with the K^+-substitution amount increasing. It reveals that the mobility of oxygen increase in $La_{2-x}K_xCuO_4$ catalysts, which enhance their catalytic activities for simultaneous removal of NO_x and soot. The last one is that the nanoparticle $La_{2-x}K_xCuO_4$ perovskite-like oxides were obtained. The good contact between soot particle and catalyst surface is indispensable conditions for an active catalyst to play an important role in soot combustion. The primary particle size of soot is 25 nm, which is much larger than the pore diameter of common catalysts. Thus, soot particulates cannot enter their inter pore. It is envisaged that in the catalytic oxidation of soot only the outer surface of the catalysts plays an important role, as only the outer surface can provide the necessary solid–solid contact. Surface atoms on surface of nanometric catalysts have extra and high surface free energies and they have good mobility. Thus, the contact is still very good between catalysts and soot even under loose contact conditions. Nanometric $La_{1.5}K_{0.5}CuO_4$ catalyst which has the maximal oxygen vacancy concentration gives the optimal catalytic activity among these samples. T_{10}, T_{50}, T_{90} are 376, 438, 487 °C and P_{N_2} is 22%, respectively, for simultaneous removal of NO_x and soot particulates under loose contact conditions between the catalyst and soot.

4. Conclusions

The nanometric $La_{2-x}K_xCuO_4$ perovskite-like complex oxides have good catalytic performances for simultaneous removal of NO_x and diesel soot particulates under loose contact conditions. In the $La_{2-x}K_xCuO_4$ catalysts, the partial substitution of K for La at A-site enhanced their catalytic activity which is due to the producing of Cu^{3+} and nonstoichiometry oxygen (λ). The oxygen vacancy concentration has an important effect on the catalytic activity because the oxygen vacancy is beneficial to enhance the adsorption and activation of NO or molecular oxygen. The change of λ value is consistent with that of the catalytic activity with the increase of x value. The optimal substitution amount of potassium x is equal to 0.5 among these samples.

Acknowledgements

This work was supported by the National Natural Science Foundation of China (No. 20473053), the Scientific Research Key Foundation for the Returned Overseas Chinese Scholars of State Education Ministry, and the National Basic Research Program of China (grant No. 2004CB217806).

References

[1] Z.P. Liu, S.J. Jenkins, D.A. King, J. Am. Chem. Soc. 126 (2004) 10746.
[2] J. Liu, Z. Zhao, C. Xun, A. Duan, L. Zhu, X. Wang, Appl. Catal. B 61 (2005) 39.
[3] S. Kureti, W. Weisweiler, K. Hizbullah, Appl. Catal. B 43 (2003) 281.
[4] K. Yoshida, S. Makino, S. Sumiya, G. Muramatsu, R. Helferich, SAE paper 892046 (1989).
[5] Y. Teraoka, K. Nakano, S. Kagawa, W.F. Shangguan, Appl. Catal. B 5 (1995) L181.
[6] Y. Teraoka, K. Nakano, W.F. Shangguan, S. Kagawa, Catal. Today 27 (1996) 107.
[7] S.S. Hong, G.D. Lee, Catal. Today 63 (2000) 397.
[8] D. Fino, P. Fino, G. Saracco, V. Specchia, Appl. Catal. B 43 (2003) 243.
[9] T. Miyazaki, N. Tokabuchi, M. Arita, M. Inoue, I. Mochida, Energy & Fuel 11 (1997) 832.

[10] Y. Teraoka, K. Kanada, S. Kagawa, Appl. Catal. B 34 (2001) 73.
[11] J.P.A. Neeft, M. Michiel, A. Jacob, Appl. Catal. B 8 (1996) 57.
[12] Z. Zhao, A. Obuchi, J. Oi-Uchisawa, A. Ogata, S. Kushiyama, Chem. Lett. 4 (1998) 367.
[13] X.G. Peng, L. Manna, W.D. Yang, J. Wickham, E. Scher, A. Kadavanich, A.P. Alivisatas, Nature 404 (2000) 59.
[14] M. Li, H. Schnablegger, S. Mann, Nature 402 (1999) 393.
[15] D.C. Hairis, T.A. Hewton, J. Solid State Chem. 69 (1987) 182.
[16] Z. Zhao, Y. Wu, Y. Yang, Sci. China 40 (1997) 464.
[17] Z. Zhao, Y. Yamada, A. Ueda, H. Sakurai, T. Kobayashi, Catal. Today 93–95 (2004) 163.
[18] R. Spencci, A. Tofanari, Catal. Today 8 (1990) 475.